The Process of Macrophage Migration Promotes Matrix Metalloproteinase-Independent Invasion by Tumor Cells

Romain Guiet, Emeline van Goethem, Céline Cougoule, Stephanie Balor, Annie Valette, Talal Al Saati, Clifford Lowell, Véronique Le Cabec, Isabelle Maridonneau-Parini

Published in final edited form as:
J Immunol. 2011 October 1; 187(7): 3806–3814. doi:10.4049/jimmunol.1101245.

The Process of Macrophage Migration Promotes Matrix Metalloproteinase-Independent Invasion by Tumor Cells

Romain Guiet[*,†], **Emeline Van Goethem**[*,†], **Céline Cougoule**[*,†], **Stéphanie Balor**[‡], **Annie Valette**[§], **Talal Al Saati**[¶], **Clifford A. Lowell**[‖,**], **Véronique Le Cabec**[*,†], and **Isabelle Maridonneau-Parini**[*,†]

[*]Centre National de la Recherche Scientifique, Institut de Pharmacologie et de Biologie Structurale, Unité Mixte de Recherche 5089, 31077 Toulouse, France

[†]Université de Toulouse, Université Paul Sabatier, Institut de Pharmacologie et de Biologie Structurale, 31062 Toulouse, France

[‡]Centre National de la Recherche Scientifique, Institut d'Exploration Fonctionnelle des Génomes, Fédération de Biologie de Toulouse, Institut de Biologie Cellulaire et de Génétique, 31062 Toulouse, France

[§]Centre de Ressources Technologiques pour Recherches Interdisciplinaires autour du Vivant, Institut des Technologies Avancées en Science du Vivant, UMS3039, Innovations pour l'Etude de la Prolifération en 3D, 31000 Toulouse, France

[¶]Institut National de la Santé et de la Recherche Médicale UMRS1043/UMR5282, Université Paul Sabatier, Centre National de la Recherche Scientifique, 31024 Toulouse, France

[‖]Department of Pathology, University of California, San Francisco, San Francisco, CA 94143

[**]Department of Laboratory Medicine, University of California, San Francisco, San Francisco, CA 94143

Abstract

Tumor-associated macrophages are known to amplify the malignant potential of tumors by secreting a variety of cytokines and proteases involved in tumor cell invasion and metastasis, but how these macrophages infiltrate tumors and whether the macrophage migration process facilitates tumor cell invasion remain poorly documented. To address these questions, we used cell spheroids of breast carcinoma SUM159PT cells as an in vitro model of solid tumors. We found that macrophages used both the mesenchymal mode requiring matrix metalloproteinases (MMPs) and the amoeboid migration mode to infiltrate tumor cell spheroids. Whereas individual SUM159PT cells invaded Matrigel using an MMP-dependent mesenchymal mode, when they were grown as

Address correspondence and reprint requests to Dr. Isabelle Maridonneau-Parini, Centre National de la Recherche Scientifique, Unité Mixte de Recherche 5089, Institut de Pharmacologie et de Biologie Structurale, 205 Route de Narbonne. 31077 Toulouse Cedex, France. isabelle.maridonneau-parini@ipbs.fr.

The online version of this article contains supplemental material.

Disclosures: The authors have no financial conflicts of interest.

spheroids, tumor cells were unable to invade the Matrigel surrounding spheroids. When spheroids were infiltrated or in contact with macrophages, tumor cell invasiveness was restored. It was dependent on the capacity of macrophages to remodel the matrix and migrate in an MMP-independent mesenchymal mode. This effect of macrophages was much reduced when spheroids were infiltrated by Matrigel migration-defective $Hck^{-/-}$ macrophages. In the presence of macrophages, SUM159PT migrated into Matrigel in the proximity of macrophages and switched from an MMP-dependent mesenchymal migration to an amoeboid mode resistant to protease inhibitors. Thus, in addition to the well-described paracrine loop between macrophages and tumor cells, macrophages can also contribute to the invasiveness of tumor cells by remodeling the extracellular matrix and by opening the way to exit the tumor and colonize the surrounding tissues in an MMP-dispensable manner.

Tumor-associated macrophages (TAMs) and the factors they release have been shown to amplify various aspects of cancer, including downregulation of adaptive immune responses, stimulation of tumor progression, and formation of metastases (1–6). Clinical evidence is substantial that, in the majority of cases, a correlation exists between macrophage density and poor patient prognosis (1); that ablation of macrophage population by genetic and pharmacological approaches can counter subsequent cancer development (7–9); and that inhibition of macrophage recruitment can enhance tumor sensitivity to radiation (10).

In the relationship between macrophages and tumor cells, cytokines, growth factors (such as epidermal growth factor and CSF-1), and proteolytic cascades are essential for successful invasion (3, 6, 11–14). Although the role of cytokines has been extensively studied, that of proteases is less well understood (3–6, 15). Proteases play a critical role at multiple stages in the metastatic cascade, including the invasion and intravasation steps, and macrophages have been shown to be the major cell type that supplies proteases to the tumor environment (3, 12, 13, 16). Proteases can facilitate tumor cell motility by cleaving components of cell-cell junctions, such as E-cadherin, and degrading components of the extracellular matrices (ECMs) and basement membrane (14, 16, 17). Regarding the role of proteases in cancer, matrix metalloproteinases (MMPs) have received most of the attention (13), but the lysosomal protease cathepsins, mostly released by macrophages, have also recently been shown to have a critical function in tumor growth and invasiveness, as well as in activation of growth factors and cytokines by cleavage of prodomains (12, 16).

TAMs have been observed at strategic positions inside tumors: They localize to areas of tumor invasion and are often found in the perivascular areas where cancer cell intravasation into the blood or lymphatic circulation occurs preferentially (12, 15, 18). In these areas, a high frequency of tumor cell movement was observed in association with macrophages, with frequent contacts between the two cell types (8). We have recently elucidated the migration characteristic of macrophages in in vitro experiments, using reconstituted three-dimensional ECMs. Macrophages use either the mesenchymal or the amoeboid migration mode, depending on the matrix architecture encountered (19). The amoeboid migration mode is characterized by a rounded or slightly protrusive cell shape, involvement of the Rho/ROCK pathway, and the lack of strong adhesive interaction and of proteolytic degradation of the matrix. The mesenchymal mode is characterized by strong adhesive interaction with the

matrix, an elongated cell shape, long F-actin rich cell protrusions, proteolytic degradation, and remodeling of the matrix under the control of Hck and dispensable Rho/ROCK pathway (19–21). To date, however, neither the mode of migration used by macrophages in a tumor environment nor the consequences of macrophage migration and matrix remodeling for the invasive capacity of tumor cells have been studied. Because it is technically difficult to address these questions in vivo, we used tumor cell spheroids, a well-established three-dimensional model of tumors (22–28). As the accumulation of TAMs in breast carcinomas has been unequivocally correlated with a poor prognosis (1), the human breast tumor cell line SUM159PT was used.

Materials and Methods

Reagents

The mixture of protease inhibitors (PIs) was composed of E64c (100 μM), aprotinin (0.04 TIU/ml), leupeptin (6 μM), pepstatin (2 μM), and GM6001 (5 μM), as described (19). Y27632 was used at 10 μM. DMSO was used as a control in all experiments. Matrigel was purchased from BD Biosciences (San Jose, CA). Pepsin-extracted collagen I (Nutragen) was obtained from Nutacon (Leimuiden, The Netherlands), CellTracker Red CMPTX and Alexa 488-phalloidin were from Invitrogen (Cergy Pontoise, France), and DAPI was from Sigma-Aldrich (St. Louis, MO).

Tumor cells and spheroid culture

The invasive human breast tumor cell line SUM159PT was cultured in F12HAM medium (Life Technologies, Carlsbad, CA) supplemented with 5% FCS, 100 U/ml penicillin (Life Technologies), 100 mg/ml streptomycin (Life Technologies), 2 μM glutamine (Life Technologies), 2 mg/ml hydrocortisone (Sigma-Aldrich), and 0.1 U/ml insulin (Novo Nordisk, Bagsvaerd, Denmark) (29). The noninvasive human breast tumor cell line T47D was cultured in RMPI 1640 medium (Life Technologies) supplemented with 5% FCS, 100 U/ml penicillin (Life Technologies), 100 μg/ml streptomycin (Life Technologies), 2 mM glutamine (Life Technologies), and 0.1 U/ml insulin (Novo Nordisk). Spheroids were generated by the hanging drop technique (30). Briefly, 24-well tissue culture plates were coated with 500 μl of 2% agar per well. The human breast tumor cell line SUM159PT was harvested and 10^3 cells/20 μl plated in the lid of tissue culture plates. After 7 d, each spheroid was transferred into wells with 500 ml culture medium. Preliminary studies have established that after 20– 24 d of culture for SUM159PT and after 12–14 d of culture for T47D, spheroids reached a diameter of ∼400 μm.

Isolation and differentiation of human monocyte-derived macrophage and mouse bone marrow-derived macrophages, staining, and coculture with spheroids

Human macrophages derived from blood monocytes and mouse bone marrow-derived macrophages (BMDMs) were differentiated as described (19, 21). Cell staining was performed using the cell-live permeant probe CellTracker Red CMPTX (Molecular Probes, Invitrogen) at 0.5 μM in PBS, as described by the manufacturer. CellTracker staining was stable for at least 15 d. Human macrophages and BMDMs both at day 7 of differentiation

were distributed (10^4 cells) into agar-coated wells containing a single spheroid and coincubated for 3 d.

Quantification of macrophage infiltration into spheroids

Formalin-fixed spheroids stained with DAPI were imaged in chambers (CoverWell PCI-1.0; Grace Bio-Labs, Bend, OR) using a Leica SP5 microscope (Leica Microsystems, Deerfield, IL) with a multiphoton source at 715 nm (coherent Chameleon) for z-stack acquisition of DAPI and CellTracker fluorescence (z-step, 1.2 μm). With the cell counter plugin of ImageJ software (National Institutes of Health, Bethesda, MD), CellTracker-stained macrophages associated to spheroids were counted. Macrophages were classified “out of spheroids” when located in the first line of nuclei and “inside” when inside the first line of nuclei. At least three spheroids per condition were used.

Migration assay

Macrophages and tumor cells were serum starved for at least 2 h. Cells harvested by Trypsin-EDTA (Life Technologies) were seeded on top of the matrix at 10^4 cells per Transwell insert. Inhibitors were placed on top of the matrix 30 min before adding the cells and in the lower chamber at the same concentrations to allow for an optimal repartition of the inhibitors within the matrix. For comigration experiments, macrophages were plated 48 h before tumor cells. After 24 h of comigration, two fields of two wells were analyzed using the motorized stage of an inverted video microscope (Leica DMIRB) and the Metamorph software. Pictures were taken automatically with a 10× objective and at constant 15-μm intervals, and cells on top and within the matrix were counted using the cell counter plugin of the ImageJ software. Tumor cells were distinguished from CellTracker-stained macrophages. In experiments using GM6001, SUM159PT cells were pre-treated for 1 h with 10 μM before their transfer to the migration chamber. Quantification was performed as previously described. The percentage of migration was obtained as the ratio of cells within the matrix to the total number of counted cells (19).

Cell morphology quantification

Cell morphologies were quantified using ImageJ and the same pictures as for migration measurement. The cell aspect ratio is the ratio of the length of the major cell axis to the minor axis, as described previously (19). For an amoeboid cell, the aspect ratio was <2.5; for intermediate morphology, the aspect ratio was >2.5 and <4.5; and for mesenchymal cells, the aspect ratio was >4.5. For each condition, ≥100 cells were scored, and a minimum of three independent experiments were analyzed.

Three-dimensional invasion assay of spheroids

Control and macrophage-infiltrated spheroids were washed and embedded in collagen I or Matrigel. Briefly, 50 μl matrix was laid down in 96-well tissue culture plates, and spheroids were resuspended at 4°C in 50 ml matrix, which was consecutively polymerized at 37°C. Brightfield pictures were registered using a Nikon eclipse TS100. Using ImageJ software, cells outside spheroids were counted, and the maximal distances covered by invasive cells were measured. The areas occupied by spheroids were measured as the difference between

day 0 and day 7. In some experiments, drugs were added into Matrigel before its polymerization and renewed in the medium every 2 d.

Video microscopy

Life-act-Cherry–expressing macrophages (20) infiltrating spheroids were visualized using a Zeiss 710 NLO with a DPPS-laser 561 nm. With use of a Lab-Tek in a CO_2 and heat-regulated chamber, cells were imaged every 15 min for 16 h.

Spheroids infiltrated with CellTracker-stained macrophages were embedded into Matrigel in a Lab-Tek chamber. Image acquisition was performed with a Zeiss 710 NLO, using a multiphoton Coherent Chameleon Vision II at 715 nm. Using a CO_2 and heat-regulated chamber, cells were imaged every 5 min for 16 h.

Histological analyses

For histomorphological analysis and immunohistochemistry assay, formalin-fixed spheroids were embedded in agarose and processed for routine histopathologic examination. Sections were stained with H&E for histomorphological analyses. Immunostaining of spheroids was preceded by the Ag retrieval technique by heating paraffin sections of spheroids in 10 mM citrate buffer, pH 6, for 10 min, except for CD68 staining, which was preceded by a pretreatment using trypsin digestion.

Immunohistochemical staining of paraffin sections of spheroids was performed with Abs directed against laminin (L9393; Sigma-Aldrich), fibronectin (F3648; Sigma-Aldrich), collagen IV (Clone CIV22; Dako, Trappes, France), collagen I (COL-1; Abcam), and macrophage CD68 (PG-M1; Dako). Spheroid sections were incubated with biotin-conjugated Abs followed by the streptavidin–biotin–peroxidase complex (ABC) method (Vector Laboratories, Burlingame, CA) and then were counterstained with hematoxylin. Negative controls were incubated in buffered solution without primary Ab.

Transmission electron microscopy

Spheroids were fixed overnight at 4°C with 2.5% glutaraldehyde and 2.5% formaldehyde (EMS; Delta-Microscopies, Ayguesvives, France) in 0.1 M cacodylate buffer, pH 7.2, and postfixed at room temperature with 1% OsO_4. The samples were then dehydrated in a graded ethanol series and embedded in Epon. The resin was polymerized for 48 h at 60°C. Sections were cut on a Leica Ultracut microtome, and ultrathin sections were mounted on 200 mesh onto Formvar-carbon–coated copper grids. Thin sections were stained with 1% uranyl acetate and lead citrate and examined at 80 kV on a JEOL 1200-EX electron microscope at the Institut Fédératif de Recherche 109 electron microscopy facility (Toulouse, France).

Scanning electron microscopy

The collagen I matrix was fixed using 0.1 M sodium cacodylate buffer supplemented with 2.5% (v/v) glutaraldehyde and prepared as previously described (19) for observation with a JEOL (Tokyo, Japan) JSM-6700F scanning electron microscope.

Statistical analyses

Each condition was performed in duplicate or triplicate; *n* = number of independent experiments. Data are reported as mean ±SD. Statistical comparisons were performed with a Student unpaired *t* test or with ANOVA (one-way ANOVA and Tukey posttest, for more than two conditions). The *p* values <0.05 are represented by one asterisk, 0.01 by two asterisks, and 0.001 by three asterisks.

Results

Macrophages infiltrate tumor cell spheroids by combining amoeboid and MMP-dependent mesenchymal migration modes

Because the presence of TAMs in breast carcinomas is associated with a poor prognosis (1), spheroids were generated using the invasive breast carcinoma cell line SUM159PT. Spheroids used in our experiments had a mean diameter of 450 ± 16 μm. They were organized according to the typical spheroid architecture (28), defined by an outer shell of proliferating cells not tightly adhering to each other and a region of packed cells, presumably corresponding to quiescent cells, that surrounds the necrotic area, observed with H&E staining (Fig. 1A) and transmission electron microscopy (TEM) images (Fig. 1B). After 3 d of spheroid/macrophage coculture, macrophages were found to infiltrate spheroids up to the necrotic core, as observed by immunohistological analysis (CD68 Abs; Fig. 1A) and by TEM (Fig. 1B). The presence of ECM proteins was also investigated in spheroids (Fig. 1A). Fibronectin was abundant, laminin and collagen IV were also present, and collagen I was absent. These ECM proteins had a heterogeneous arrangement, either filling or not filling intercellular spaces. Thus, the structure of SUM159PT spheroids mimics in vivo breast tumors, in which the presence of these proteins has been documented (31).

Next, we stained macrophages with CellTracker to quantify this infiltration in spheroids, using multiphoton microscopy (Fig. 1C–E). As shown in Fig. 1E, macrophages efficiently infiltrated spheroids. To characterize the mesenchymal and amoeboid modes, PI mix (containing the pan-MMP inhibitor GM6001 and inhibitors mostly dedicated to lysosomal proteases [LyPIs]) and the Rho-kinase (ROCK) inhibitor Y27632 were respectively used as previously described (19). In the presence of PI mix or Y27632, the percentage of macrophages (Fig. 1E) infiltrating spheroids was significantly decreased. When GM6001 was used alone, it affected the infiltration of macrophages with the same efficiency as PI mix, whereas no inhibitory effect was obtained with LyPI (Fig. 1E), indicating that macrophage infiltration into spheroids was mostly dependent on MMPs. Finally, when PIs and Y27632 were combined, their effects were additive, indicating that infiltration of macrophages into spheroids relied on the two migration modes identified so far. By time-lapse video microscopy, we recorded macrophages with representative morphologies migrating to different depths of spheroids—that is, a macrophage with a typically elongated mesenchymal morphology (Supplemental Fig. 1, arrowhead) and a more rounded macrophage (arrow), both cells having F-actin–rich cell protrusions at the front, similar to three-dimensional podosomes (Supplemental Fig. 1; Ref. 20). Contrary to the ECM we used previously, which promoted one or the other migration mode (19), we have been able to obtain the two migration modes when macrophages migrated into a matrix of intermediate

properties of architecture and viscoelasticity, that is, collagen I at 3.6 mg/ml polymerized as a “gel” (Supplemental Fig. 2A, 2B). In this environment, when PIs and Y27632 were combined, their effects were additive (Supplemental Fig. 2C), and the percentage of cells with an intermediate morphology between mesenchymal and amoeboid was increased (Supplemental Fig. 2D). Thus a combination of the migration modes could exist in three-dimensional environments, such as spheroids characterized by heterogeneous architecture and/or intermediate rheological properties.

From these results, we conclude that macrophages infiltrate spheroids via both the mesenchymal and the amoeboid modes. The use of the two modes could be reproduced in an ECM with heterogeneous architecture and intermediate viscoelastic properties. In marked contrast to our previous data showing that the mesenchymal mode used by macrophages in ECM is MMP independent (19), in this work we show that the use of the mesenchymal mode to infiltrate SUM159PT cell spheroids is MMP dependent.

Macrophages infiltrating multicellular tumor spheroids trigger the invasion of tumor cells into the surrounding matrix

To explore tumor cell invasiveness, spheroids were embedded into Matrigel, an ECM extracted from a mouse sarcoma, mostly containing laminin and collagen IV. As shown in Fig. 2A, in the absence of macrophages, SUM159PT cells did not escape from spheroids into the surrounding matrix, with only some small outgrowths appearing at the surface of spheroids (Fig. 2A), suggesting that Matrigel might form a barrier around spheroids, as previously described (32). This finding was not due to a migration defect of our cell line because, as described earlier (29), individualized SUM159PT cells were competent to infiltrate Matrigel (see below). When spheroids were embedded into fibrillar collagen I, SUM159PT rapidly invaded the matrix (Supplemental Fig. 3A), as previously observed (33). Interestingly, we found that the presence of infiltrated macrophages in spheroids conferred an invasive phenotype to the tumor cells in Matrigel (Fig. 2A), indicating that macrophages can trigger the egress of tumor cells from spheroids. In fact, both SUM159PT and CellTracker-stained macrophages were found to invade the Matrigel (Fig. 2B). Similarly, macrophages stimulated the egress of cells when spheroids were made with the breast epithelial tumor cell line T47D (data not shown). In contrast, in fibrillar collagen I, the presence of macrophages in spheroids did not enhance matrix invasion (Supplemental Fig. 3B). The impact of macrophages on Matrigel invasion by tumor cells was quantified by measuring (1) the surface occupied by the spheroids, (2) the number of cells out of spheroids, and (3) the maximal invasion distance reached by cells (Fig. 2C). All three parameters were found to be dramatically increased when macrophage-infiltrated spheroids were compared with spheroids without macrophages (Fig. 2D).

Thus, as reported in vivo, we have established an in vitro system in which macrophages can stimulate tumor cell invasiveness.

Tumor cell invasion requires macrophage proximity and protease activity

To characterize the effect of macrophages on the invasive phenotype of tumor cells, spheroids infiltrated by CellTracker-stained macrophages were examined by time-lapse

fluorescence microscopy after embedding into Matrigel. As illustrated in Videos 1–4, we observed that macrophages were the first to leave the spheroids (Supplemental Video 1); they infiltrated Matrigel with back-and-forth movements, making iterative contacts with other macrophages or with SUM159PT cells (Fig. 3A; Supplemental Video 2) localized at the periphery of the spheroid. Those tumor cells that invaded the matrix were often in proximity to macrophages (Fig. 3B; Supplemental Video 3) and frequently migrated as groups of a few cells (Supplemental Video 4). These observations led us to examine whether a direct contact between macrophages and spheroids was required to trigger tumor cell invasion. As shown in Fig. 3C, with the use of Transwell cultures, spheroids were embedded in Matrigel either without (a) or with (b) infiltrated macrophages. Alternatively, with the use of noninfiltrated spheroids, macrophages were layered either in the lower chamber (c) or in the upper chamber, atop the matrix (d). Under this last condition, once macrophages had reached spheroids (data not shown), tumor cells started to invade the matrix, resulting in an intermediate result between the spheroids containing macrophages and those without (Fig. 3D). When macrophages were trapped in the lower chamber (c), spheroids behaved like spheroids without macrophages and tumor cells did not invade the matrix (Fig. 3D). From these results, we conclude that a direct contact of macrophages with the spheroids is required to promote tumor cell invasiveness.

Next, using spheroids infiltrated by macrophages embedded into Matrigel, we examined the role of proteases in the process of matrix invasion. In the presence of GM6001, cellular invasion of the matrix was decreased (Fig. 3E), suggesting that the exit of macrophages from spheroids might be inhibited by GM6001, and, as a consequence, cell invasion was reduced. In fact, when GM6001 was added during the macrophage infiltration process of spheroids, a large proportion of macrophages remained at the spheroid periphery (see Fig. 1E), and this did not result in an inhibition of the invasion of Matrigel when the drug was no longer present at the second stage (Fig. 3E). Moreover, when GM6001 was present during both macrophage infiltration and cell invasion, a marginal inhibitory effect was obtained, suggesting that macrophages located at the periphery of spheroids are the main actor of invasion. When LyPI, which inhibits macrophage migration in Matrigel, was added during the invasion process, both the number of cells out of spheroids and the distance covered by invasive cells were decreased (Fig. 3E). The following observations were made: (1) Tumor cells are unable to invade Matrigel around spheroids in the absence of macrophages; (2) GM6001 inhibits macrophage migration inside spheroids and inhibits spheroid invasiveness (Fig. 3E); and (3) Ly-PI inhibits macrophage migration in Matrigel (Ref. 19; Supplemental Fig. 4) and inhibits spheroid invasiveness. Taken together, these observations suggest that both sets of proteases are involved in macrophage-triggered tumor cell invasiveness. Actually, the combination of GM6001 and LyPI resulted in a strong inhibition of the invasion process (Fig. 3E).

In conclusion, the capacity of macrophages to promote the invasion of a Matrigel matrix by SUM159PT cells grown as spheroids requires proximity of the two cell types and relies on a protease-dependent process.

In the presence of macrophages, tumor cells switch to the amoeboid mode to invade Matrigel

Next, we explored the role of proteases in tumor cell invasiveness triggered by macrophages. First, we studied the effect of the various PIs on the mobility of SUM159PT cells seeded on the top of a thick layer of Matrigel polymerized in Transwells (19). As shown in Fig. 4A, SUM159PT cells infiltrated the matrix in an MMP-dependent manner because GM6001 strongly decreased the percentage of invasive cells, whereas neither LyPI nor Y27632 affected SUM159PT cell migration. We thus concluded that these tumor cells used the mesenchymal mode and MMPs, rather than the amoeboid migration mode, to infiltrate Matrigel. Moreover, because the addition of Y27632 to GM6001 did not potentiate the inhibitory effect of GM6001, SUM159PT cells apparently cannot operate the mesenchymal to amoeboid shift that has been described for some tumor cells migrating into collagen I (34–36). As previously reported, the migration of human macrophages was affected only by LyPI, confirming that they use only the mesenchymal migration mode in Matrigel and not MMPs (Supplemental Fig. 4A; Ref. 19). Thus, both macrophages and SUM159PT migrated into Matrigel using the mesenchymal mode, but distinct sets of proteases.

Second, macrophages and tumor cells were seeded together on the top of Matrigel, and their respective migration capacities were analyzed. Of interest, the distance of migration covered by tumor cells was increased to a level comparable to that of macrophages (Fig. 4B, 4C). Although the presence of tumor cells did not detectably influence the distance covered by migrating macro-phages(Fig. 4B, 4C), the percentage of migrating cells slightly increased (Supplemental Fig. 4A, 4B). The presence of tumor cells did not change the susceptibility of macrophages to the drugs (Supplemental Fig. 4B), and as previously reported, macrophages formed tunnels into Matrigel (Supplemental Fig. 4C; Ref. 20). In contrast, the susceptibility of tumor cells was markedly modified: SUM159PT cells became insensitive to GM6001 and sensitive to Y27632 treatment (Fig. 4D). Tumor cells were found to migrate in proximity to macrophages (Fig. 4E, 4F), potentially in the tunnels formed by macrophages (Fig. 4G), where tumor cells might use the amoeboid migration mode. LyPI had no effect on the percentage of migrating SUM159PT cells (Fig. 4D) but inhibited macrophage migration in Matrigel (Supplemental Fig. 4A, 4B), and this coincided with a shortening of the migration distance covered by tumor cells (data not shown).

In sum, these results show that SUM159PT cells can adapt their migration capacity to the environment because a portion of the tumor cells took advantage of the presence of macrophages by switching to the amoeboid migration mode. Consequently, the maximal distance covered by tumor cells was markedly increased, matching that of macrophages.

$Hck^{-/-}$ macrophages with defective Matrigel migration are less effective in triggering tumor cell invasiveness

Finally, we evaluated the role played by the process of macrophage migration in promoting the migration of tumor cells away from spheroids into the surrounding Matrigel matrix. To avoid the use of drugs, we took advantage of $Hck^{-/-}$ BMDMs, which have a reduced migration capacity (∼50%) in Matrigel (21). Hck, a tyro-sine kinase specifically expressed

in phagocytes, is involved in lysosome exocytosis (37–39) and in mesenchymal migration of macrophages, which depends on lysosomal proteases (21). *Hck*$^{-/-}$ macrophages were found to infiltrate spheroids as well as those with a *wt* genotype (Fig. 5A), which could be expected because *Hck*$^{-/-}$ macrophages show normal expression and activity of MMPs (21). When macrophage-infiltrated spheroids were embedded into Matrigel, we observed that, in the presence of *Hck*$^{-/-}$ macrophages, invasion of the matrix and the distance covered by invading cells were reduced, compared with spheroids infiltrated by *wt* macrophages (Fig. 5B, 5C). These results further support the idea that the process of macrophage migration is in itself required to facilitate the invasive capacity of tumor cells in Matrigel.

Discussion

Our understanding of the role of TAMs is progressing, but some aspects are not yet elucidated. This challenge must be met, given the critical importance of these cells at multiple stages of cancer progression and the therapeutic potential of pharmacologically controlling macrophage infiltration in tumors.

The first set of data concerns the observation that macrophages use a combination of amoeboid and mesenchymal modes to infiltrate three-dimensional tumor cell spheroids. We have previously shown that the architecture of extracellular matrices dictates the migration mode used by human macrophages (19); in porous matrices they use the amoeboid mode, and in nonporous gel-like matrices, the mesenchymal mode. In a tumor cell environment, macrophages are likely adapting their migration mode to the heterogeneous surroundings they encounter in spheroids, which comprise large and tight intercellular spaces more or less filled with ECM proteins. In Supplemental Fig. 1, a macrophage infiltrating a cell spheroid (arrow) adopts an intermediate phenotype, with F-actin accumulating at the tip of a cell protrusion and a more rounded cell shape than the macrophage deeply infiltrated in the spheroid (arrowhead). The use of the two migration modes could also be obtained in a gelled collagen I matrix that combined porous and dense areas. In this matrix, a significant proportion of macrophages exhibited intermediate cell shape, between rounded and elongated. Thus, macrophages could alternatively use the two migration modes, switching from one to the other with a transition phenotype in the middle. Otherwise, they could use a migration mode at a transition stage between amoeboid and mesenchymal movements, combining proteolytic degradation of the matrix at the tip of three-dimensional podosomes (19, 20) with ROCKmediated actomyosin contraction and rounded cell shape. Further work will be necessary to distinguish between these two hypotheses. We also found that, to infiltrate spheroids, macrophages require MMPs, whereas these proteases are dispensable for macrophage mesenchymal migration inside ECMs (Ref. 19; Supplemental Fig 4). Among the numerous substrates of MMPs (40), proteolysis of adhesion receptors might be critical in opening cell–cell junctions to allow the migration of macrophages into spheroids. Thus, macrophages are able to sense the extracellular environment, adapt their migration mode (19), and, possibly, differentially deliver proteases. Whether different sets of proteases are either differentially secreted or indiscriminately released by macrophages remains to be determined. Whether MMPs are released by macrophages, by tumor cells, or by both also has to be elucidated.

The second set of data concerns the effect of macrophages on the invasive capacity of tumor cells. Because the density and composition of the ECM are modified in most tumors (41, 42), we thought that Matrigel, which is extracted from a mouse sarcoma, was well adapted in our study to mimic the tumor environment. In contrast to fibrillar collagen I, the invasive tumor cells SUM159PT did not efficiently abandon the spheroid environment to penetrate the Matrigel, suggesting that it might form a sort of barrier around spheroids. SUM159PT cells have actually accomplished the epitheliomesenchymal transition (29), a switch considered instrumental for the invasion phenotype. We show that individual SUM159PT cells are able to infiltrate Matrigel, but when these cells form a spheroid they lose this property. The presence of macrophages inside spheroids was not an absolute requisite because tumor cell invasiveness was also initiated when macrophages reached spheroids from outside or were maintained at the periphery of spheroids by MMP inhibitors. In addition to the well-described contribution of various cytokines released by macrophages and tumor cells to facilitate the invasive phenotype (3–6), we report that the macrophage migration capacity is also involved in that process by itself. In our spheroid model, we observed that macrophages, migrating into Matrigel in an MMP-independent mesenchymal mode, were frequently in direct contact with those tumor cells that were at the edge of spheroids, presumably in the process of exit. Furthermore, tumor cells that were in the process of invading the matrix individually or collectively were often found to move forward close to macrophages. Macrophages are professional migrating cells capable of moving in every type of body tissue and across anatomic boundaries. The proximity of macrophages thus probably constitutes an opportunity for tumor cells, which might be less well equipped for transtissular migration. In the presence of $Hck^{-/-}$ macrophages, which have a reduced capacity to migrate inside Matrigel, tumor cell invasiveness was found to be reduced, further supporting the notion that the macrophage migration process in itself facilitates tumor cell invasion, although we cannot exclude that $Hck^{-/-}$ macrophages have another undiscovered deficiency that could also affect tumor cell migration. When SUM159PT cells were layered on Matrigel in the absence of macrophages, they infiltrated the matrix using the mesenchymal migration mode, in an MMP-dependent manner. In the presence of macrophages, however, they used the amoeboid mode, and their migration distance increased to match that covered by macrophages. We propose that the matrix remodeling activity of macrophages, which combines proteolytic degradation with ingestion and compaction of the matrix to form tunnels, as described earlier (20), probably helps tumor cells to tube travel (43–45) and migrate independently of their own proteolytic activity. The advantages of using the amoeboid migration mode compared with the mesenchymal mode might be related to a rapid movement of the cells (46). Moreover, one can hypothesize that slipping into tunnels is less energy consuming than digging holes. The failure of MMP inhibitors to prevent cancer progression in clinical trials (47), and in particular the proposal that MMP-independent amoeboid migration of tumor cells might be relevant in vivo (44), lead us to propose that tumor cells could actually follow macrophages using the amoeboid mode. In vitro, fibro-blasts have been noted to form tracks in the ECM, enabling noninvasive cancer cells to migrate collectively, whereas invasive cancer cells with mesenchymal characteristics invaded the matrix equally well in the presence or in the absence of fibroblasts (48). Thus, it is likely that both fibroblasts and macrophages, two

components of the tumoral microenvironment, facilitate tumor progression, although their respective importance remains to be established.

In conclusion, we report that macrophages infiltrate tumor spheroids using both the mesenchymal and the amoeboid migration modes and that mesenchymal migration in cellular and noncellular three-dimensional environments requires distinct sets of proteases. In addition to the well-described paracrine loop between tumor cells and macrophages, which enhances tumor cell migration, the macrophage matrix remodeling activity is also involved in the process of tumor cell invasion. This work describes a new role for macrophages in tumor progression and points out that effectors of macrophage mesenchymal migration such as Hck, a phagocyte-specific protein, are potential antitumoral targets.

Supplementary Material

Refer to Web version on PubMed Central for supplementary material.

Acknowledgments

We thank Etienne Joly for critical reading of the manuscript, Florence Capilla for immunohistochemistry experiments, Renaud Poincloux and Brice Ronsin for Toulouse-réseau-d'imagerie facilities, Fabienne Gauffre for rheological measurements, and Catherine Muller-Staumont for providing SUM159PT cells.

This work was supported in part by Association pour la Recherche sur le Cancer 2010-120-1733 and Association pour la Recherche sur le Cancer Equipement No. 8505 and Agence Nationale de la Recherche 2010-01301 and by Fondation pour la Recherche Médicale (to R.G.) and La Ligue contre le Cancer (to E.V.G.).

References

1. Bingle L, Brown NJ, Lewis CE. The role of tumour-associated macrophages in tumour progression: implications for new anticancer therapies. J Pathol. 2002; 196:254–265. [PubMed: 11857487]
2. Condeelis J, Pollard JW. Macrophages: obligate partners for tumor cell migration, invasion, and metastasis. Cell. 2006; 124:263–266. [PubMed: 16439202]
3. Joyce JA, Pollard JW. Microenvironmental regulation of metastasis. Nat Rev Cancer. 2009; 9:239–252. [PubMed: 19279573]
4. Pollard JW. Trophic macrophages in development and disease. Nat Rev Immunol. 2009; 9:259–270. [PubMed: 19282852]
5. DeNardo DG, Andreu P, Coussens LM. Interactions between lymphocytes and myeloid cells regulate pro- versus anti-tumor immunity. Cancer Metastasis Rev. 2010; 29:309–316. [PubMed: 20405169]
6. Mantovani A, Sica A. Macrophages, innate immunity and cancer: balance, tolerance, and diversity. Curr Opin Immunol. 2010; 22:231–237. [PubMed: 20144856]
7. Lin EY, Nguyen AV, Russell RG, Pollard JW. Colony-stimulating factor 1 promotes progression of mammary tumors to malignancy. J Exp Med. 2001; 193:727–740. [PubMed: 11257139]
8. Qian B, Deng Y, Im JH, Muschel RJ, Zou Y, Li J, Lang RA, Pollard JW. A distinct macrophage population mediates metastatic breast cancer cell extravasation, establishment and growth. PLoS ONE. 2009; 4:e6562. [PubMed: 19668347]
9. Meng Y, Beckett MA, Liang H, Mauceri HJ, van Rooijen N, Cohen KS, Weichselbaum RR. Blockade of tumor necrosis factor alpha signaling in tumor-associated macrophages as a radiosensitizing strategy. Cancer Res. 2010; 70:1534–1543. [PubMed: 20145121]

10. Ahn GO, Tseng D, Liao CH, Dorie MJ, Czechowicz A, Brown JM. Inhibition of Mac-1 (CD11b/CD18) enhances tumor response to radiation by reducing myeloid cell recruitment. Proc Natl Acad Sci USA. 2010; 107:8363–8368. [PubMed: 20404138]
11. DeNardo DG, Barreto JB, Andreu P, Vasquez L, Tawfik D, Kolhatkar N, Coussens LM. CD4(+) T cells regulate pulmonary metastasis of mammary carcinomas by enhancing protumor properties of macrophages. Cancer Cell. 2009; 16:91–102. [PubMed: 19647220]
12. Gocheva V, Wang HW, Gadea BB, Shree T, Hunter KE, Garfall AL, Berman T, Joyce JA. IL-4 induces cathepsin protease activity in tumor-associated macrophages to promote cancer growth and invasion. Genes Dev. 2010; 24:241–255. [PubMed: 20080943]
13. Kessenbrock K, Plaks V, Werb Z. Matrix metalloproteinases: regulators of the tumor microenvironment. Cell. 2010; 141:52–67. [PubMed: 20371345]
14. Mason SD, Joyce JA. Proteolytic networks in cancer. Trends Cell Biol. 2011; 21:228–237. [PubMed: 21232958]
15. Wyckoff J, Wang W, Lin EY, Wang Y, Pixley F, Stanley ER, Graf T, Pollard JW, Segall J, Condeelis J. A paracrine loop between tumor cells and macrophages is required for tumor cell migration in mammary tumors. Cancer Res. 2004; 64:7022–7029. [PubMed: 15466195]
16. Gocheva V, Joyce JA. Cysteine cathepsins and the cutting edge of cancer invasion. Cell Cycle. 2007; 6:60–64. [PubMed: 17245112]
17. Rowe RG, Weiss SJ. Breaching the basement membrane: who, when and how? Trends Cell Biol. 2008; 18:560–574. [PubMed: 18848450]
18. Wyckoff JB, Wang Y, Lin EY, Li JF, Goswami S, Stanley ER, Segall JE, Pollard JW, Condeelis J. Direct visualization of macrophage-assisted tumor cell intravasation in mammary tumors. Cancer Res. 2007; 67:2649–2656. [PubMed: 17363585]
19. Van Goethem E, Poincloux R, Gauffre F, Maridonneau-Parini I, Le Cabec V. Matrix architecture dictates three-dimensional migration modes of human macrophages: differential involvement of proteases and podosome-like structures. J Immunol. 2010; 184:1049–1061. [PubMed: 20018633]
20. Van Goethem E, Guiet R, Balor S, Charrière GM, Poincloux R, Labrousse A, Maridonneau-Parini I, Le Cabec V. Macrophage podosomes go 3D. Eur J Cell Biol. 2011; 90:224–236. [PubMed: 20801545]
21. Cougoule C, Le Cabec V, Poincloux R, Al Saati T, Mège JL, Tabouret G, Lowell CA, Laviolette-Malirat N, Maridonneau-Parini I. Three- dimensional migration of macrophages requires Hck for podosome organization and extracellular matrix proteolysis. Blood. 2010; 115:1444–1452. [PubMed: 19897576]
22. Bingle L, Lewis CE, Corke KP, Reed MW, Brown NJ. Macrophages promote angiogenesis in human breast tumour spheroids in vivo. Br J Cancer. 2006; 94:101–107. [PubMed: 16404363]
23. Choi MR, Stanton-Maxey KJ, Stanley JK, Levin CS, Bardhan R, Akin D, Badve S, Sturgis J, Robinson JP, Bashir R, et al. A cellular Trojan Horse for delivery of therapeutic nanoparticles into tumors. Nano Lett. 2007; 7:3759–3765. [PubMed: 17979310]
24. Drenkard D, Becke FM, Langstein J, Spruss T, Kunz-Schughart LA, Tan TE, Lim YC, Schwarz H. CD137 is expressed on blood vessel walls at sites of inflammation and enhances monocyte migratory activity. FASEB J. 2007; 21:456–463. [PubMed: 17167064]
25. Spoettl T, Hausmann M, Menzel K, Piberger H, Herfarth H, Schoelmerich J, Bataille F, Rogler G. Role of soluble factors and three-dimensional culture in in vitro differentiation of intestinal macrophages. World J Gastroenterol. 2007; 13:1032–1041. [PubMed: 17373737]
26. Lin RZ, Chang HY. Recent advances in three-dimensional multicellular spheroid culture for biomedical research. Biotechnol J. 2008; 3:1172–1184. [PubMed: 18566957]
27. Friedrich J, Seidel C, Ebner R, Kunz-Schughart LA. Spheroid-based drug screen: considerations and practical approach. Nat Protoc. 2009; 4:309–324. [PubMed: 19214182]
28. Hirschhaeuser F, Menne H, Dittfeld C, West J, Mueller-Klieser W, Kunz-Schughart LA. Multicellular tumor spheroids: an underestimated tool is catching up again. J Biotechnol. 2010; 148:3–15. [PubMed: 20097238]
29. Flanagan L, Van Weelden K, Ammerman C, Ethier SP, Welsh J. SUM-159PT cells: a novel estrogen independent human breast cancer model system. Breast Cancer Res Treat. 1999; 58:193–204. [PubMed: 10718481]

30. Lobjois V, Frongia C, Jozan S, Truchet I, Valette A. Cell cycle and apoptotic effects of SAHA are regulated by the cellular microenvironment in HCT116 multicellular tumour spheroids. Eur J Cancer. 2009; 45:2402–2411. [PubMed: 19553104]
31. Bergamaschi A, Tagliabue E, Sørlie T, Naume B, Triulzi T, Orlandi R, Russnes HG, Nesland JM, Tammi R, Auvinen P, et al. Extracellular matrix signature identifies breast cancer subgroups with different clinical outcome. J Pathol. 2008; 214:357–367. [PubMed: 18044827]
32. Olsen CJ, Moreira J, Lukanidin EM, Ambartsumian NS. Human mammary fibroblasts stimulate invasion of breast cancer cells in a three-dimensional culture and increase stroma development in mouse xenografts. BMC Cancer. 2010; 10:444. [PubMed: 20723242]
33. Sabeh F, Shimizu-Hirota R, Weiss SJ. Protease-dependent versus -independent cancer cell invasion programs: three-dimensional amoeboid movement revisited. J Cell Biol. 2009; 185:11–19. [PubMed: 19332889]
34. Friedl P, Wolf K. Proteolytic and non-proteolytic migration of tumour cells and leucocytes. Biochem Soc Symp. 2003:277–285. [PubMed: 14587300]
35. Friedl P. Prespecification and plasticity: shifting mechanisms of cell migration. Curr Opin Cell Biol. 2004; 16:14–23. [PubMed: 15037300]
36. Sanz-Moreno V, Marshall CJ. The plasticity of cytoskeletal dynamics underlying neoplastic cell migration. Curr Opin Cell Biol. 2010; 22:690–696. [PubMed: 20829016]
37. Cougoule C, Carréno S, Castandet J, Labrousse A, Astarie-Dequeker C, Poincloux R, Le Cabec V, Maridonneau-Parini I. Activation of the lysosome-associated p61Hck isoform triggers the biogenesis of podosomes. Traffic. 2005; 6:682–694. [PubMed: 15998323]
38. Hirahashi J, Mekala D, Van Ziffle J, Xiao L, Saffaripour S, Wagner DD, Shapiro SD, Lowell C, Mayadas TN. Mac-1 signaling via Src-family and Syk kinases results in elastase-dependent thrombohemorrhagic vasculopathy. Immunity. 2006; 25:271–283. [PubMed: 16872848]
39. Guiet R, Poincloux R, Castandet J, Marois L, Labrousse A, Le Cabec V, Maridonneau-Parini I. Hematopoietic cell kinase (Hck) isoforms and phagocyte duties—from signaling and actin reorganization to migration and phagocytosis. Eur J Cell Biol. 2008; 87:527–542. [PubMed: 18538446]
40. Gialeli C, Theocharis AD, Karamanos NK. Roles of matrix metalloproteinases in cancer progression and their pharmacological targeting. FEBS J. 2011; 278:16–27. [PubMed: 21087457]
41. Levental KR, Yu H, Kass L, Lakins JN, Egeblad M, Erler JT, Fong SF, Csiszar K, Giaccia A, Weninger W, et al. Matrix crosslinking forces tumor progression by enhancing integrin signaling. Cell. 2009; 139:891–906. [PubMed: 19931152]
42. Parekh A, Weaver AM. Regulation of cancer invasiveness by the physical extracellular matrix environment. Cell Adh Migr. 2009; 3:288–292. [PubMed: 19458499]
43. Wolf K, Mazo I, Leung H, Engelke K, von Andrian UH, Deryugina EI, Strongin AY, Bröcker EP, Friedl P. Compensation mechanism in tumor cell migration: mesenchymal-amoeboid transition after blocking of pericellular proteolysis. J Cell Biol. 2003; 160:267–277. [PubMed: 12527751]
44. Wyckoff JB, Pinner SE, Gschmeissner S, Condeelis JS, Sahai E. ROCK- and myosin-dependent matrix deformation enables protease-independent tumor-cell invasion in vivo. Curr Biol. 2006; 16:1515–1523. [PubMed: 16890527]
45. Friedl P, Wolf K. Tube travel: the role of proteases in individual and collective cancer cell invasion. Cancer Res. 2008; 68:7247–7249. [PubMed: 18794108]
46. Berton S, Belletti B, Wolf K, Canzonieri V, Lovat F, Vecchione A, Colombatti A, Friedl P, Baldassarre G. The tumor suppressor functions of p27(kip1) include control of the mesenchymal/amoeboid transition. Mol Cell Biol. 2009; 29:5031–5045. [PubMed: 19596789]
47. Coussens LM, Fingleton B, Matrisian LM. Matrix metalloproteinase inhibitors and cancer: trials and tribulations. Science. 2002; 295:2387–2392. [PubMed: 11923519]
48. Gaggioli C, Hooper S, Hidalgo-Carcedo C, Grosse R, Marshall JF, Harrington K, Sahai E. Fibroblast-led collective invasion of carcinoma cells with differing roles for RhoGTPases in leading and following cells. Nat Cell Biol. 2007; 9:1392–1400. [PubMed: 18037882]

Abbreviations used in this article

BMDM	bone marrow-derived macrophage
ECM	extracellular matrix
LyPI	lysosomal protease inhibitor
MMP	matrix metalloproteinase
PI	protease inhibitor
TAM	tumor-associated macrophage
TEM	transmission electron microscopy

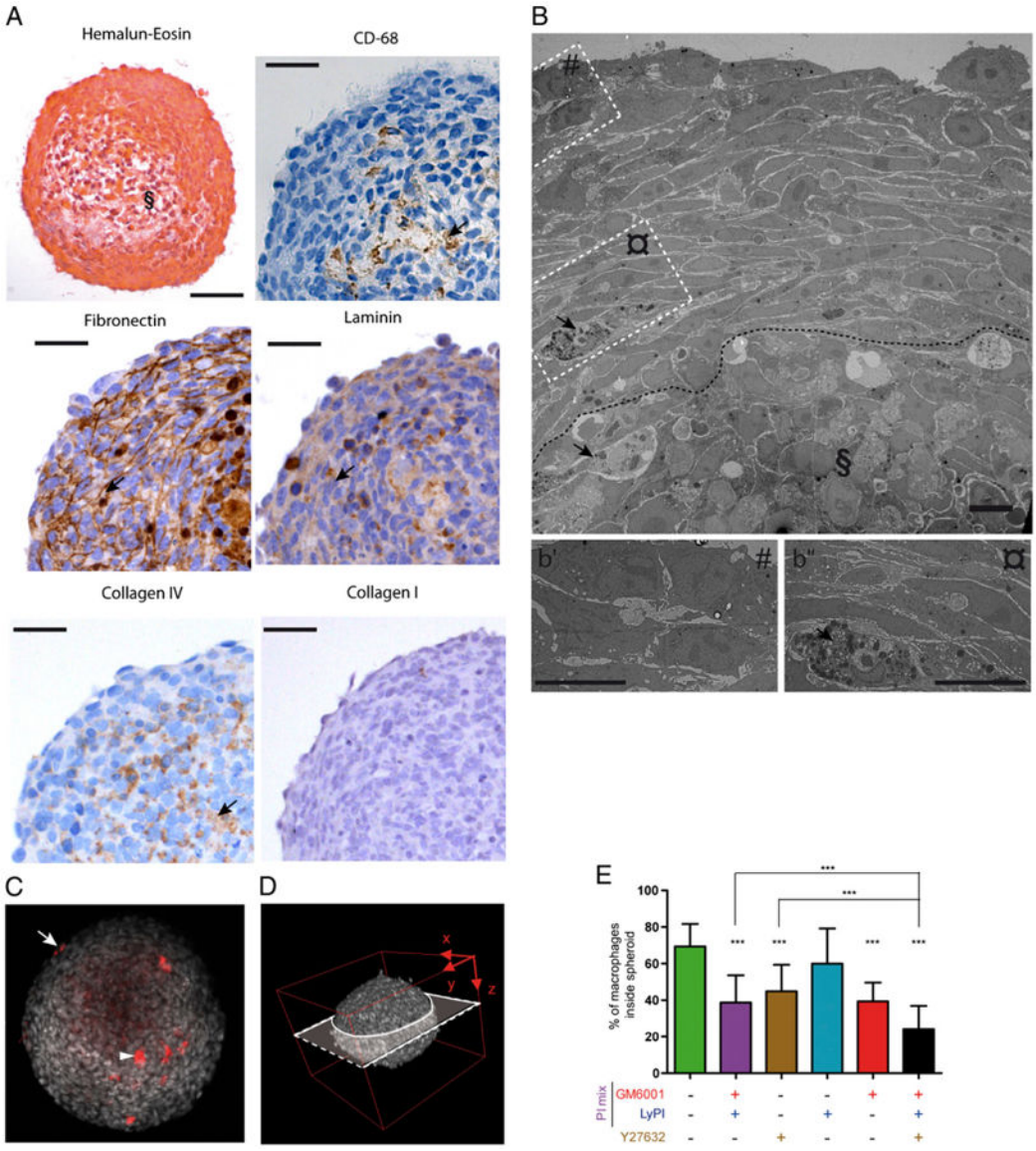

Figure 1.

Human macrophages infiltrate tumor cell spheroids, using the mesenchymal and amoeboid migration modes. SUM159PT cell spheroids were coincubated for 3 d with CellTracker-stained macrophages, with or without drugs. *A*, Cross sections of paraffin-embedded spheroids stained with H&E (§ indicates the apoptotic/necrotic core; scale bars, 100 μm) or immunohistochemically stained with Abs directed against CD68, laminin, fibronectin, collagen IV, or collagen I (scale bars, 50 μm). *B*, TEM image of an ultrathin section of a macrophage-infiltrated spheroid; *insets* are magnified as b′ and b″; § indicates the apoptotic/necrotic core delineated by a dotted line (scale bars, 10 μm). Arrows in *A* (CD-68 staining) and *B* show infiltrated macrophages. Arrows in *A* show significant staining of fibronectin, laminin, and collagen IV. *C* and *D*, Multiphoton acquisition (original magnification ×90) of DAPI-stained spheroids infiltrated by CellTracker-stained macrophages. *C*, A spheroid cross section set in the three-dimensional spheroid reconstitution in *D* is shown. The arrowhead

and arrow indicate a CellTracker-stained macrophage located inside and outside the spheroid, respectively. *E*, Quantification of macrophage infiltration into spheroids, with or without inhibitors. Results are expressed as the percentage of macrophages inside spheroids (100% corresponds to macrophages inside plus macrophages at the periphery). Results are expressed as mean ± SD ($n = 3$). ***$p < 0.001$.

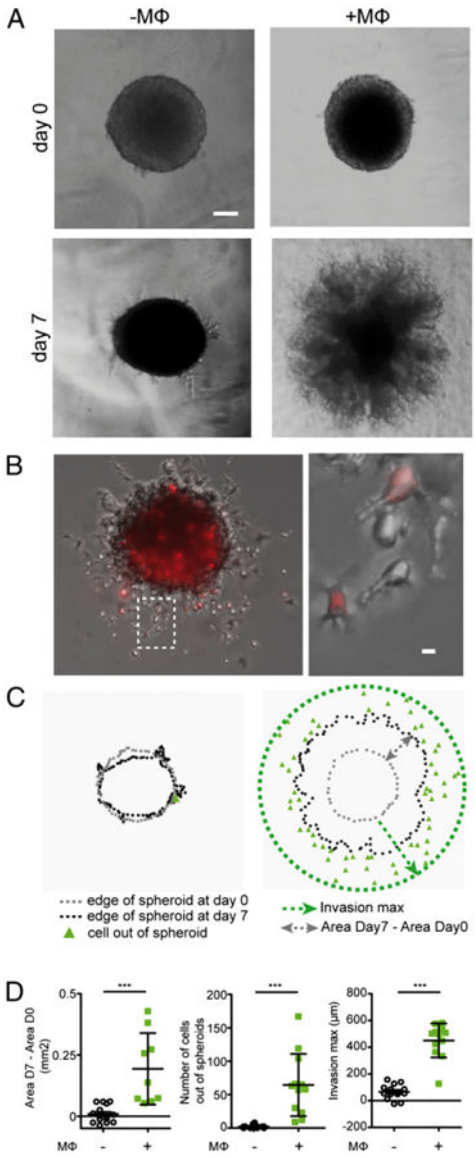

Figure 2.

Human macrophages infiltrated into spheroids trigger tumor cell invasion into Matrigel. *A*, Brightfield images of spheroids (*left panels*, –MΦ) and human macrophage-infiltrated spheroids (*right panels*, +MΦ) embedded into Matrigel. In the presence of macrophages, tumor cells invade the matrix. Scale bar, 100 µm. *B*, Spheroids coincubated with Cell-Tracker-stained human macrophages, then embedded into Matrigel. After 48 h, a fluorescence image shows that macrophages (red) and tumor cells invade the matrix. The *left panel* is a higher magnification, denoted by the dashed box in the *right panel*. Scale bar, 10 µm. *C*, Schematic presentation of invasion quantification: The spheroid size is measured at day 0 (gray dots) and day 7 (black dots); the maximal invasion distance (dotted green line) is quantified as shown by the green arrow, and the number of cells outside spheroids (represented by green triangles) is counted. *D*, Invasion parameters show that macrophages significantly enhanced invasion. Results are expressed as mean ± SD ($n = 3$). ***$p < 0.001$.

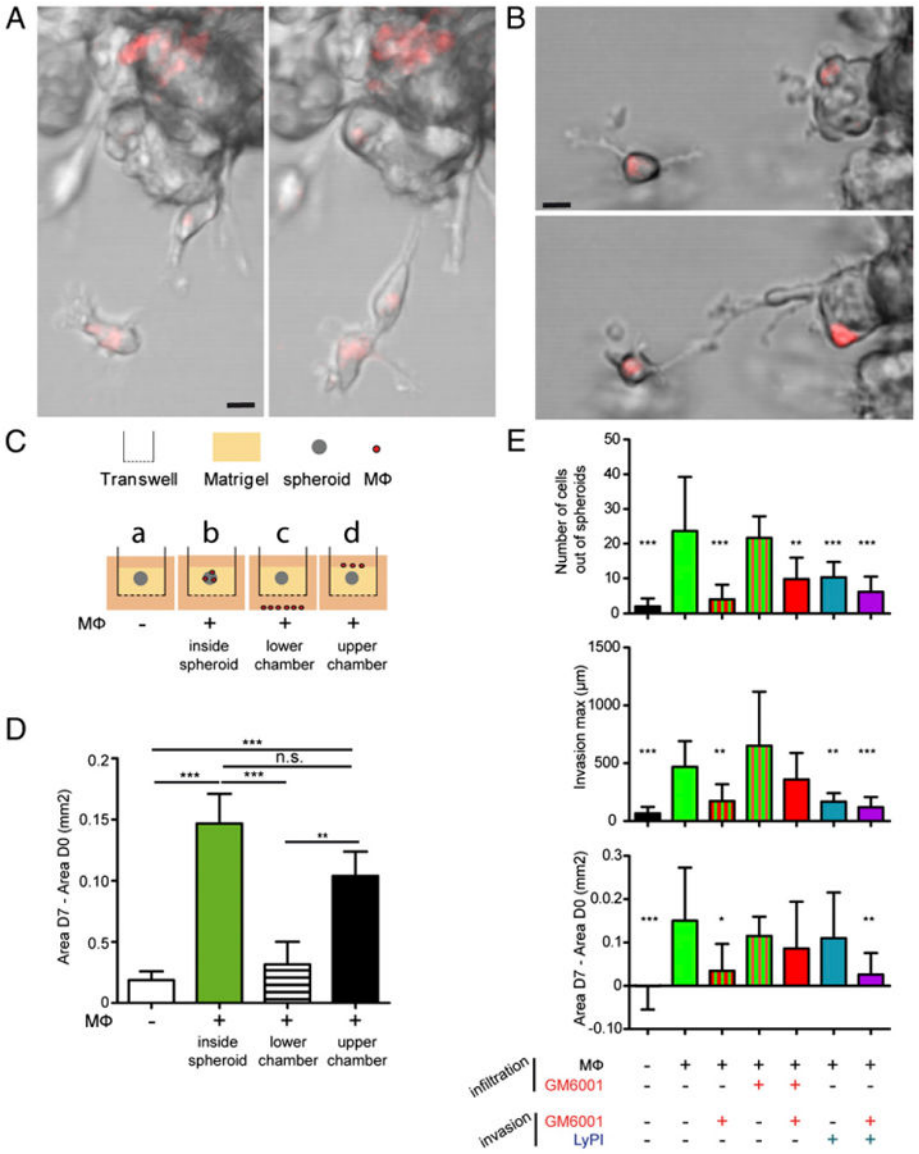

Figure 3.

Tumor cell invasion requires macrophage vicinity and proteases. *A* and *B*, Spheroids infiltrated by CellTracker-stained macrophages were embedded into Matrigel, and time-lapse microscopy allowed visualization of cell movements. Scale bar, 10 µm. *C*, A schematic presentation of the protocol used is shown. Spheroids (*a*) and macro-phage-infiltrated spheroids (*b*) were embedded into a thick layer of Matrigel. Macrophages were also layered in the lower chamber of the-Transwell (*c*) or seeded on the top of Matrigel in the upper chamber (*d*). In this latter case, macrophages infiltrated Matrigel and reached spheroids after 3–4 d. *D*, Quantification of invasion under the experimental conditions depicted in *A*. *E*, PIs were added or not, as indicated: during the macrophage infiltration process of spheroids (infiltration) and/or during the invasion assay when spheroids were embedded into Matrigel (invasion). Results are expressed as mean ± SD ($n = 3$). *$p < 0.05$, **$p < 0.01$, ***$p < 0.001$.

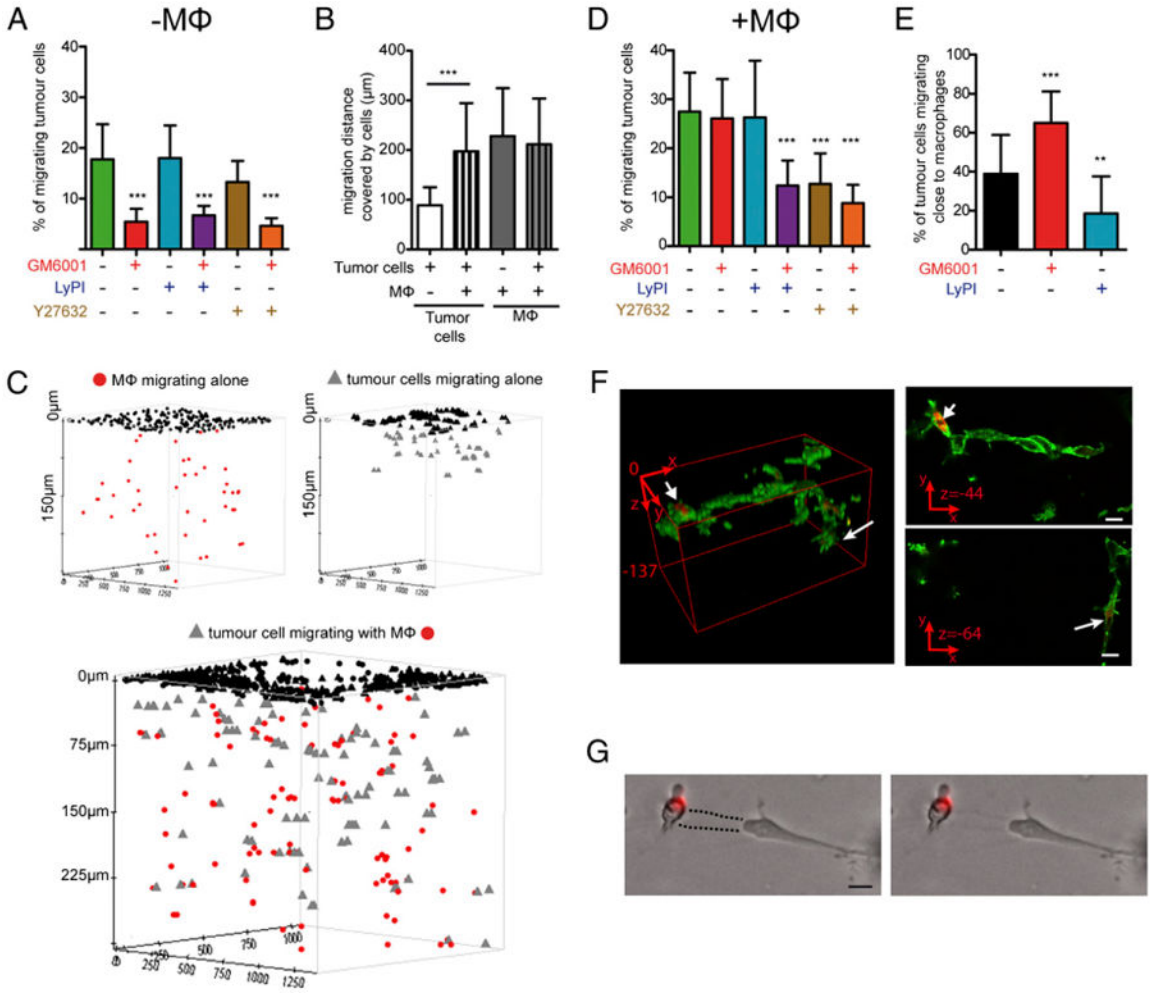

Figure 4.

In the presence of macrophages, Matrigel invasion by tumor cells is no longer sensitive to MMP inhibition. SUM159PT cells were seeded on thick layers of Matrigel polymerized in Transwells in the presence of inhibitors, with or without macrophages. *A*, Tumor cells were inhibited only by GM6001. *B*, The maximal migration distance covered by SUM159PT cells increased in the presence of human macrophages. ***$p < 0.001$. *C*, Three-dimensional positions of macrophages and/or tumor cells migrating in Matrigel is represented using Topcat software (black symbols: noninfiltrated cells at the top of the matrix). *D*, Tumor cells comigrating with macrophages are not inhibited by GM6001 but are affected by Y27632. *E*, The percentage of tumor cells close to macrophages in Matrigel increased with GM6001 and decreased with LyPi. ***$p < 0.001$, **$p < 0.01$. *F*, CellTracker-stained macrophages and SUM159PT cells were fixed, stained with Alexa 488-phalloïdine, and visualized into Matrigel using a Zeiss 710 NLO (137 z-sections of 1 µm). *Left panel*, Three-dimensional reconstitution. *Upper right panel* and *lower right panels*, Tumor cells in contact with CellTracker-stained macrophages, with a characteristic mesenchymal morphology at different depths into the matrix (arrows). Scale bars, 10 µm. *G*, Overlay of fluorescence and brightfield images shows comigration of tumor cells and CellTracker-stained macrophages

in a tunnel (dotted line on the *left image*). Scale bar, 10 μm. Results are expressed as mean ± SD (n = 3).

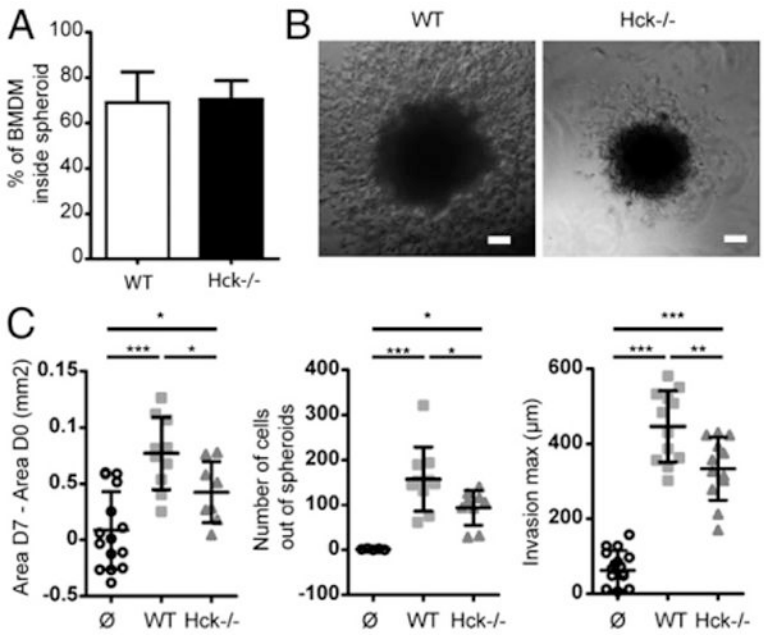

Figure 5.

Hck$^{-/-}$ macrophages, deficient for Matrigel migration, are less effective at promoting tumor cell invasiveness. *A*, Spheroids were coincubated with CellTracker-stained *wt* or *Hck*$^{-/-}$ macrophages for 3 d, and the number of macrophages associated with spheroids was counted on 30 z-sections of 1.2 µm. *B*, Spheroids infiltrated by *wt* or *Hck*$^{-/-}$ BMDMs for 3 d were embedded into Matrigel. After 7 d, brightfield images of cells invading Matrigel are shown. Scale bars, 100 µm. *C*, Invasion parameters show that cell invasion is decreased with *Hck*$^{-/-}$ macrophages compared with *wt*. Results are expressed as mean ± SD ($n = 3$). *$p <$ 0.05, **$p < 0.01$, ***$p < 0.001$.